


III–V-on-silicon anti-colliding pulse-type mode-locked laser

View metadata, citation and similar papers at core.ac.uk

brought to you by  CORE

provided by Ghent University Academic Bibliography

S. KEIVANIAN,¹ S. OVI,¹ M. TASSARI,² Z. WANG,³ X. FU,⁴ S. LATKOWSKI,⁵ S. MARIEN,⁶ L. THOMASSEN,⁴ F. LELARGE,⁵ G. DUAN,⁵ G. LEPAGE,⁶ P. VERHEYEN,⁶ J. VAN CAMPENHOUT,⁶ E. BENTE,³ AND G. ROELKENS^{1,2,3,*}

¹Photonics Research Group, Department of Information Technology, Ghent University–IMEC, Ghent B-9000, Belgium

²Center for Nano- and Biophotonics (NB-Photonics), Ghent University, Ghent B-9000, Belgium

³Photonic Integration Group, Eindhoven University of Technology, Den Dolech 2, Eindhoven, The Netherlands

⁴Antwerp Space, Berkenrodelei 33, 2260 Hoboken, Belgium

⁵III–V lab, a joint lab of “Alcatel-Lucent Bell Labs France,” “Thales Research and Technology” and “CEA Leti,” Campus Polytechnique, 1, Avenue A. Fresnel, 91767 Palaiseau cedex, France

⁶IMEC, Kapeldreef 75, B-3001 Leuven, Belgium

⁷Currently at Calioipa–Huawei, Ghent B-9000, Belgium

*Corresponding author: gunther.roelkens@intec.ugent.be

Received 13 March 2015; revised 28 May 2015; accepted 2 June 2015; posted 3 June 2015 (Doc. ID 236136); published 23 June 2015

An anti-colliding pulse-type III–V-on-silicon passively mode-locked laser is presented for the first time based on a III–V-on-silicon distributed Bragg reflector as outcoupling mirror implemented partially underneath the III–V saturable absorber. Passive mode-locking at 4.83 GHz repetition rate generating 3 ps pulses is demonstrated. The generated fundamental RF tone shows a 1.7 kHz 3 dB linewidth. Over 9 mW waveguide coupled output power is demonstrated. © 2015 Optical Society of America

OCIS codes: (060.5625) Radio frequency photonics; (250.5300) Photonic integrated circuits; (140.4050) Mode-locked lasers.

<http://dx.doi.org/10.1364/OL.40.003057>

Mode-locked lasers provide a means of generating pure microwave signals that are essential in microwave photonic applications [1]. Passively mode-locked devices are of great interest since no RF signal needs to be provided to drive the laser: it generates a pulse train, the repetition rate of which is determined by the length of the laser cavity. Output power and the purity of the RF spectrum are of great importance in microwave photonic applications. In [2], an anti-colliding pulse mode-locked laser design is proposed, where the saturable absorber is implemented on the low-reflectivity outcoupling mirror of the laser cavity. The theoretical analysis of such a cavity under passive mode-locking points to higher output power, lower timing jitter, and better RF spectral purity compared to standard self-colliding pulse designs, where the saturable absorber is implemented next to the high-reflectivity mirror. Recently, this was also experimentally observed in III–V semiconductor devices [3]. In this Letter, we report the realization of an anti-colliding pulse-type mode-locked laser on a

III–V-on-silicon platform for the first time. The implementation on this platform allows to easily fabricate distributed Bragg reflectors in the silicon device layer enabling the integration of these devices with other optical components. It also allows using low-loss silicon waveguide structures (both in terms of linear scattering losses as well as nonlinear two-photon absorption losses) to form the laser cavity, which positively affects the RF linewidth and optical output power. Moreover, the compatibility of the silicon photonics platform with high-volume manufacturing as well as the potential to co-integrate high-speed optical modulators and germanium photodetectors, make the integration of a mode-locked laser on a silicon photonics platform very attractive for microwave photonics. First demonstrations of low-phase-noise III–V-on-silicon mode-locked lasers were based on classical colliding ring cavity and self-colliding linear cavity arrangements. In this case, using stabilization of a linear cavity arrangement mode-locked laser through external optical feedback, 15 kHz 3 dB RF linewidth was obtained at 9.95 GHz repetition rate [4]. Recently, we also demonstrated ring cavity and linear cavity devices on our III–V-on-silicon platform, with a 12 kHz 3 dB RF linewidth, without stabilization using an external Fabry–Perot cavity [5]. The novel anti-colliding pulse-type III–V-on-silicon mode-locked laser demonstrated in this work shows a 1.7 kHz 3 dB RF linewidth at 4.83 GHz, a substantial improvement over the state-of-the-art. The device geometry is shown in Figs. 1(a) and 1(b). The saturable absorber and the optical amplifier are implemented in the III–V-on-silicon waveguide section. The optical mode is then coupled to the silicon waveguide using an adiabatic taper structure. The main part of the laser cavity length is realized in the silicon waveguide layer using a spiral waveguide structure. The laser cavity mirrors are also fabricated in the silicon waveguide layer: a high reflectivity distributed Bragg reflector mirror at the right end of the laser cavity

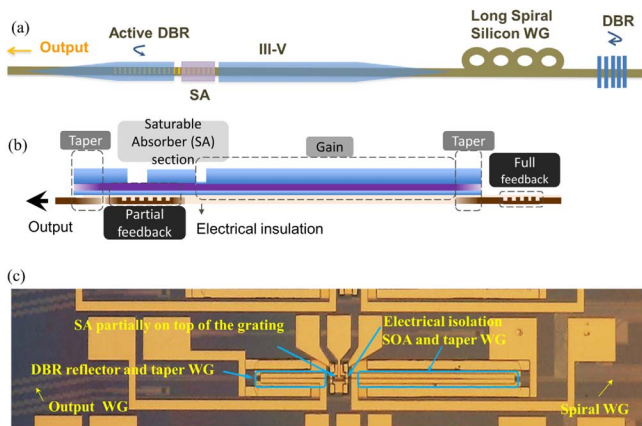


Fig. 1. Layout of the novel III-V-on-silicon mode-locked laser cavity: (a) top view; (b) longitudinal cross-section. A microscope image of the fabricated device is shown in (c).

and a lower reflectivity distributed Bragg reflector outcoupling mirror partly underneath the saturable absorber at the left end. The fabrication procedure of the 400 nm-thick silicon waveguides and the III-V waveguide structure is identical to the one described in [5]. The III-V-on-silicon integration is based on adhesive bonding using DVS-BCB [6], and the bonding layer thickness was 75 nm in this experiment. Also, the same epitaxial layer stack as described in [5] was used.

The optical coupling between the silicon device layer and the III-V waveguide layer is realized using a spotsizer converter by tapering both the III-V mesa and silicon waveguide as described in [7]. The total III-V taper length is 190 μm , tapering from 3 μm down to 0.5 μm width (using a two-step taper where the first section tapers from 3 μm to 0.9 μm over 40 μm , while the second spotsizer converter tapers down to 0.5 μm over 150 μm). The silicon waveguide tapers from 300 nm to 2 μm width over 150 μm . The III-V saturable absorber is 65 μm long, while the III-V gain section is 650 μm long (not including the 150 μm -long spotsizer converters). The confinement factor of the optical mode in the quantum wells is 7.5% both in the gain section and in the saturable absorber. The high-reflectivity cavity mirror is formed by a broadband silicon DBR grating etched 180 nm deep in the silicon waveguide layer (grating period 505 nm, 75% duty cycle, 40 μm long) providing close to 100% reflectivity. The second cavity mirror is formed by a silicon distributed Bragg reflector implemented underneath the saturable absorber. This grating has a 490 nm period, 75% duty cycle, a total length of 100 μm , and extends 40 μm under the output III-V spotsizer converter. According to simulation, this yields a peak reflectivity of 60% and a 3 dB bandwidth of 4 nm for a 75 nm-thick DVS-BCB bonding layer. The majority of the cavity length is formed by a silicon spiral waveguide of 0.7 cm length in order to reach a pulse repetition rate of about 5 GHz (4.83 GHz in the experiment). The waveguide propagation loss (650 nm-wide rib waveguides) was characterized through cut-back measurements to be 0.7 dB/cm in the 1550 nm wavelength range (TE polarization). A microscope image of the fabricated device is shown in Fig. 1(c). In order to simplify the electrical contacting, the p-contact of the output III-V spotsizer converter was connected to the p-contact of the III-V gain region. A common n-contact

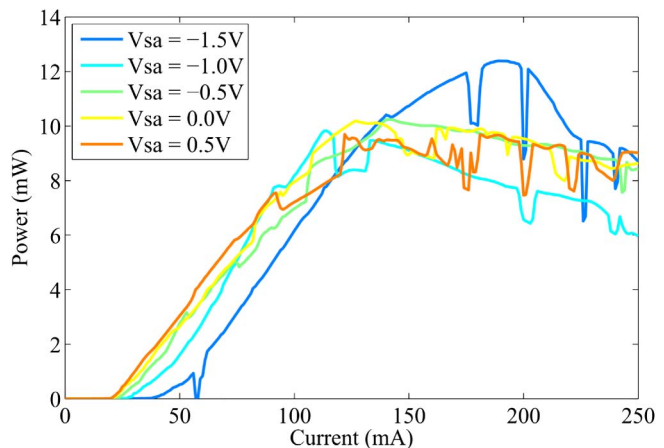


Fig. 2. Power versus current plot of the device under test as a function of saturable absorber reverse bias voltage (fiber-coupled output power)

was used. Device characterization is carried out on a thermoelectric cooler at 20°C. The light-current characteristic (fiber coupled output power) of the device is shown in Fig. 2. The output of the mode-locked laser was coupled to an optical fiber through a fiber-to-chip grating coupler, located 0.7 mm away from the laser cavity. The fiber-to-chip coupling efficiency is measured to be -12 dB. For the characterization of the passive mode-locking, a reverse bias voltage of -0.7 V was applied to the saturable absorber and 61 mA current is injected in the spotsizer converters and semiconductor optical amplifier as these settings resulted in the most flat RF spectrum of the generated pulse train. The laser threshold for this saturable absorber bias setting is 30 mA. At thermal roll-over, the waveguide coupled output power is over 9 mW for a -0.7 V reverse bias voltage on the saturable absorber, substantially higher than previously reported III-V-on-silicon mode-locked laser geometries (ring cavity and linear cavity colliding pulse lasers) with similar dimensions implemented using the same technology [6].

The dips observed in the light-current characteristics are attributed to parasitic reflections from the grating coupler used for fiber coupling. The back-reflection of the grating coupler was measured to be -17 dB. In order to reduce these reflections, a dedicated grating coupler structure can be used with -50 dB back-reflection as demonstrated in [8]. For the detailed characterization of the mode-locked laser output, the optical fiber was either connected to a high-resolution (20 MHz) optical spectrum analyzer, a high-speed photodiode (50 GHz bandwidth) that was connected to a 50 GHz electrical spectrum analyzer, or a second harmonic generation based intensity autocorrelator (after passing an EDFA). An optical isolator was used to prevent external back-reflections into the laser. The high-resolution optical spectrum is shown in Fig. 3(a), showing the 40 pm spaced longitudinal modes of the laser. A 3.5 nm 10 dB optical bandwidth is obtained. A super-modulation on the spectrum can be observed. This is attributed to parasitic reflections in the laser cavity, leading to a parasitic pulse train with the same repetition rate as the main laser pulses. The linewidth of the individual optical lines is smaller than the resolution of the spectrum analyzer (20 MHz) as shown in Fig. 3(b).

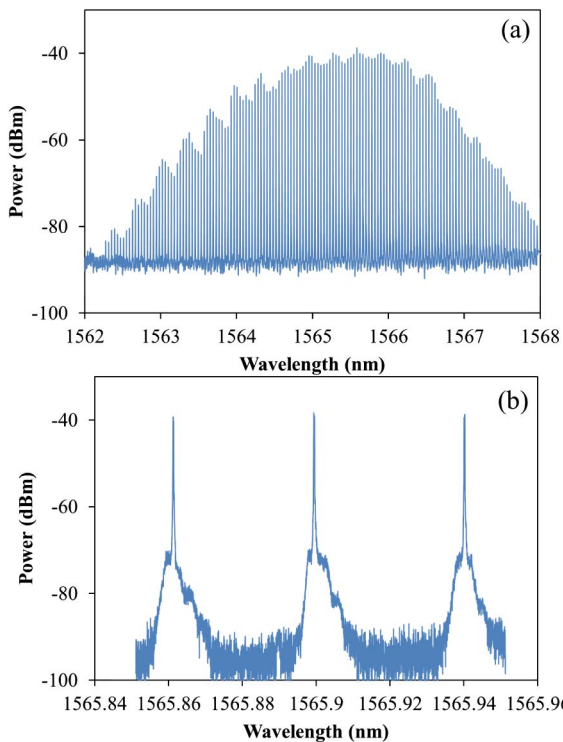


Fig. 3. (a) High-resolution optical spectrum at 61 mA drive current and -0.7 V reverse bias on the saturable absorber showing the 40 pm spaced longitudinal modes (20 MHz spectral resolution). A 10 dB optical bandwidth of 3.5 nm is obtained. (b) Zoom of the optical spectrum indicating a linewidth of the longitudinal laser modes better than 20 MHz.

The pedestals in Fig. 3(b) are attributed to intensity noise on the pulse train and the mode frequency variations that are related to that.

The intensity autocorrelator measurements shown in Fig. 4 indicate a pulse duration of 3 ps when a sech^2 pulse shape is assumed. A wide span electrical spectrum is shown in Fig. 5(a), showing both the fundamental 4.83 GHz RF tone and its harmonics. A power variation of less than 4 dB across all the recorded RF frequency comb components is obtained. The

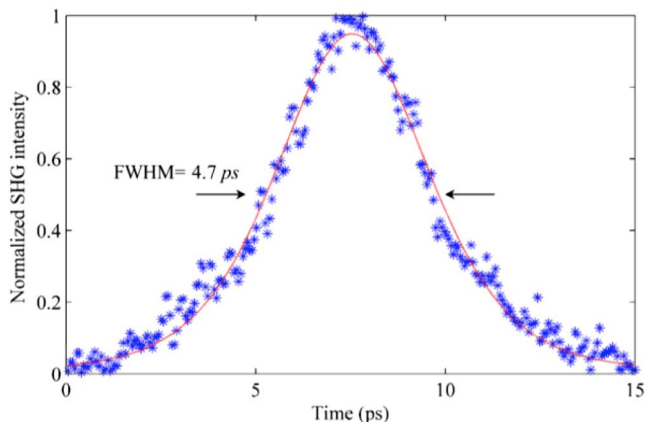


Fig. 4. Intensity autocorrelator trace (blue: experimental, red: theoretical fitting). The 4.7 ps FWHM of the trace corresponds to a 3 ps pulse width assuming its sech^2 amplitude profile.

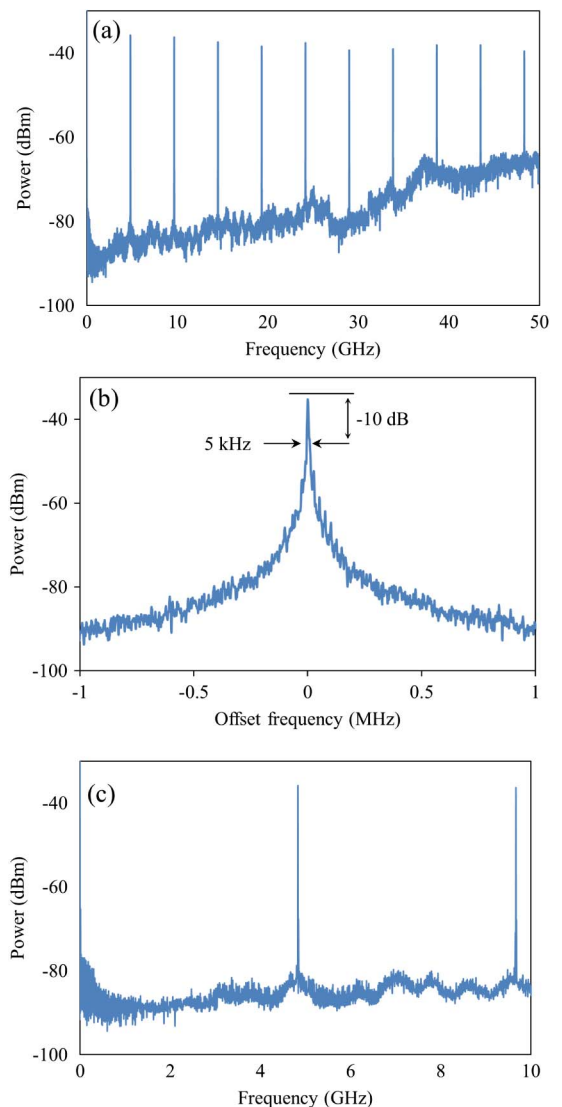


Fig. 5. (a) Wide span electrical spectrum of the generated pulse train; (b) linewidth of the fundamental RF tone; (c) zoom of the electrical spectrum from baseband to the second harmonic illustrating a clean spectrum between the RF harmonics. Resolution bandwidth and video bandwidth used to obtain the RF spectra were 500 kHz, 50 kHz for (a), 1.5 kHz, 150 Hz for (b), and 500 kHz, 50 kHz for (c), respectively.

linewidth of the fundamental RF tone is very narrow: a 1.7 kHz 3 dB linewidth (5 kHz 10 dB linewidth) is observed, as shown in Fig. 5(b). A zoom of the electrical spectrum from baseband to the second harmonic is shown in Fig. 5(c) illustrating a clean spectrum between the RF harmonics.

Finally, the phase noise spectrum of the device under passive mode-locking was measured. Figure 6 shows the phase noise spectrum of the fundamental RF tone from 100 Hz to 100 MHz from the carrier frequency. Low phase noise can be observed as expected from the anti-colliding pulse design [2]. Residual tones at 30 kHz and its harmonics can also be observed, which are attributed to the current source used to bias the gain section of the mode-locked laser. The total integrated jitter from 50 kHz to 10 MHz is 2.8 ps.

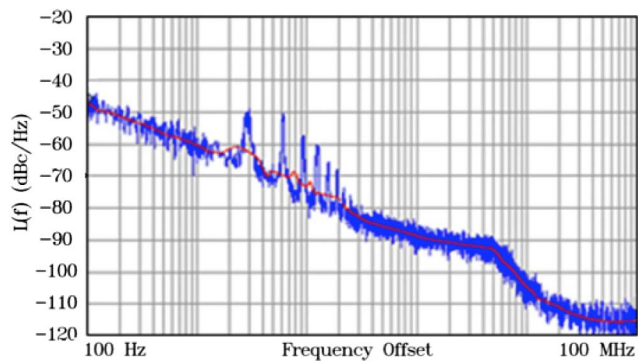


Fig. 6. Single-sideband phase noise spectrum (blue: experimental, red: average).

In conclusion, an integrated anti-colliding pulse-type mode-locked laser cavity implemented on a III-V on silicon platform is presented for the first time. Very narrow RF linewidth as well as high optical output power are obtained, making such devices promising sources for advanced microwave photonic applications.

The mode-locked laser is coupled to a silicon waveguide circuit in which other high-speed optical components can be

realized, enabling the realization of more complex photonic integrated circuits for applications in the field of microwave photonics.

European Space Agency-Electrophotonic Frequency Converter project.

REFERENCES

1. J. Yao, *J. Lightwave Technol.* **27**, 314 (2009).
2. J. Javaloyes and S. Balle, *Opt. Lett.* **36**, 4407 (2011).
3. J. Zhuang, V. Pusino, D. Ying, S. Chan, and M. Sorel, *Opt. Lett.* **40**, 617 (2015).
4. S. Srinivasan, M. Davenport, M. Heck, J. Hutchinson, E. Norberg, G. Fish, and J. Bowers, *Front. Optoelectron.* **7**, 265 (2014).
5. S. Keyvaninia, S. Uvin, M. Tassaert, X. Fu, S. Latkowski, J. Marien, L. Thomassen, F. Lelarge, G. Duan, P. Verheyen, G. Lepage, J. Van Campenhout, E. Bente, and G. Roelkens, *Opt. Express* **23**, 3221 (2015).
6. S. Keyvaninia, M. Muneeb, S. Stankovic, P. J. Van Veldhoven, D. Van Thourhout, and G. Roelkens, *Opt. Mater. Express* **3**, 35 (2013).
7. S. Keyvaninia, G. Roelkens, D. Van Thourhout, C. Jany, M. Lamponi, A. Le Liepvre, F. Lelarge, D. Make, G.-H. Duan, D. Bordel, and J.-M. Fedeli, *Opt. Express* **21**, 3784 (2013).
8. Y. Li, D. Vermeulen, Y. De Koninck, G. Yurtsever, G. Roelkens, and R. Baets, *Opt. Lett.* **37**, 4356 (2012).